

# Topographic evolution and morphology of surfaces evolving in response to coupled fluvial and hillslope sediment transport

Guy Simpson and Fritz Schlunegger<sup>1</sup>

Geology Institute, ETH Zurich, Zurich, Switzerland

Received 21 August 2002; revised 21 January 2003; accepted 11 March 2003; published 14 June 2003.

[1] This paper quantifies how the ratio of sediment transport on hillslopes to sediment transport in channels influences surface and channel network morphologies and the dynamics of topographic evolution. This problem is investigated by development and investigation of a simple deterministic model incorporating mass balance of sediment and runoff coupled with a law combining dispersive and concentrative sediment transport processes. Our analysis includes the identification of a new nondimensional parameter  $D_e$  that is a function of rainfall, system size, rock type, and hydraulic regime and that is a measure of the relative importance of fluvial and hillslope sediment transport. We show that  $D_e$  has an important influence on the surface morphology (e.g., total exposed surface area and interface width which reflects surface roughness and relief), channel network form (e.g., channel sinuosity), channel spacing, and timescale of surface evolution. Surface and channel network morphologies are also strongly influenced by the overall surface slope relative to the magnitude of initial topographic roughness. Topographic evolution occurs in distinct phases of relief growth and decay, the transition between which is controlled by a saturation phenomenon related to the growth of spatial correlations. The scaling behavior of simulated topography with respect to both time and space is obtained and is shown to be independent of  $D_e$ . Roughness exponents are found to be independent of  $D_e$  but dependent on the magnitude of initial roughness. Interface width is shown to grow and decay as a logarithm of time. **INDEX TERMS:** 1625 Global Change: Geomorphology and weathering (1824, 1886); 1815 Hydrology: Erosion and sedimentation; 1860 Hydrology: Runoff and streamflow; 3210 Mathematical Geophysics: Modeling; **KEYWORDS:** erosion, landscape, topography, drainage network, diffusion, FEM modeling

**Citation:** Simpson, G., and F. Schlunegger, Topographic evolution and morphology of surfaces evolving in response to coupled fluvial and hillslope sediment transport, *J. Geophys. Res.*, 108(B6), 2300, doi:10.1029/2002JB002162, 2003.

## 1. Introduction

[2] In recent years there has been widespread appreciation that some important aspects of landscape morphology and dynamics result from interaction between hillslopes and channel networks. Recognizing this, a number of numerical models that incorporate coupling between hillslope and channel processes have been developed [e.g., Kirkby, 1986; Ahnert, 1987; Willgoose *et al.*, 1991a; Chase, 1992; Howard, 1994]. These models have been used to explore various aspects of landscape development including general topographic evolution [e.g., Willgoose *et al.*, 1991b, 1991c; Kooi and Beaumont, 1994; Tucker and Slingerland, 1994], response to climate change [Rinaldo *et al.*, 1995; Tucker and Slingerland, 1997] and tectonics [Beaumont *et al.*, 1992; Willet *et al.*, 2001], and landscape self-organization [Rigon *et al.*, 1994]. To date, however, relatively little

detailed research based on numerical modeling has been carried out on the important aspects concerning the coupling itself that exists between hillslope and channel processes (see, however, Tucker and Bras [1998]). Thus a number of interesting and important general questions remain unresolved. For example, how does the relative importance of channel and hillslope sediment transport influence landscape and network morphologies and the timescales of landscape evolution? What parameter(s) controls channel spacing? Why are some channel networks regular with a well defined channel spacing whereas others are highly branching? This paper uses numerical modeling as a tool to explore several problems such as these.

[3] In general terms, the morphology of natural landscapes (that are not subject to lithospheric deformation) reflects the strength and nature of climatic forcing relative to the ability of topography to relax by diffusion. In a transport-limited system where erosion rates are proportional to the divergence of sediment flux, runoff from rainfall has the potential to roughen topography by channel incision due to the strong dependency of sediment flux on fluid discharge [Graf, 1971]. This generally concentrative process is counteracted by sediment transport proportional to

<sup>1</sup>Now at the Institute of Geological Sciences, University of Bern, Bern, Switzerland.

the local surface gradient [Culling, 1960] that tends to fill depressions and smooth topography. The presence of two competing classes of processes, one concentrative (and dominant in channels) associated with runoff, which causes positive feedback and the other dispersive (and dominant on hillslopes) causing negative feedback, are recognized to comprise the basic minimum requirements to explain the formation of landscapes containing convex hillslopes and incised channel networks.

[4] Importance of the balance between dispersive and concentrative transport processes in influencing landscape development is widely appreciated on the basis of field-based and experimental studies [e.g., Schumm, 1956; Dunne and Aubry, 1986; Montgomery and Dietrich, 1992; Hasbargen and Paola, 2000] and has been the focus of theoretical and numerical investigations [e.g., Smith and Bretherton, 1972; Willgoose *et al.*, 1991a, 1991b; Howard, 1994; Loewenherz-Lawrence, 1994; Smith *et al.*, 1997a, 1997b; Tucker and Bras, 1998]. For example, it is now generally accepted that instability leading to incision of an initially unchanneled surface is associated with a dominance of concentrative over dispersive processes in the transport of surface sediments. Although it was initially shown on the basis of a linear stability analysis that the shortest transverse topographic wavelengths are the fastest growing [Smith and Bretherton, 1972], implying that channels should be spaced an infinitesimal distance apart, it has since been demonstrated that nonlinear effects govern subsequent channelization leading to stable topographic surfaces with finite channel spacings [e.g., Smith *et al.*, 1997a]. An alternative interpretation is that the failure of linear models to select a finite channel spacing is an artifact due to oversimplify the equations governing surface fluid flow. For example, Izumi and Parker [1995, 2000] show that a linear analysis of the full equations of shallow overland flow coupled with erosion leads to the selection of finite channel wavelengths in reasonable agreement with observations.

[5] It is also generally accepted that the balance between dispersive and concentrative sediment transport processes is reflected in the general morphology of landscapes [e.g., Montgomery and Dietrich, 1992; Kirkby, 1994]. For example, highly incised, rough landscapes such as those found in semiarid badlands are thought to be formed by dominantly concentrative processes whereas weakly incised, smooth landscapes characteristic of more temperate humid settings are believed to be formed dominantly by dispersive sediment transport processes. However, not all hillslope processes are necessarily dispersive in nature (e.g., some forms of mass movement lead to concentrated deposits). A large amount of theoretical work has been focused on understanding how interaction between hillslope and channel processes determines landscape properties such as the contributing area-slope relationship and the drainage density [e.g., Tarboton *et al.*, 1992; Willgoose *et al.*, 1991d; Willgoose, 1994; Tucker and Bras, 1998]. Results of these studies are generally consistent with the concept of a "belt of no fluvial erosion" [Horton, 1945] extending some distance  $x_c$  down from drainage divides which is controlled by competition between hillslope and water-assisted sediment transport processes. Scaling at distances smaller than  $x_c$  is controlled by diffusive processes whereas scaling at

distances larger than  $x_c$  is controlled by fluvial processes. The distance  $x_c$  is also related to the drainage density [Tarboton *et al.*, 1992]. Thus the ratio between the magnitudes of hillslope to fluvial sediment transport is anticipated to strongly influence the drainage density. This inference is consistent with field observations showing that whereas badland drainage densities are typically on the order of 1000 km/km<sup>2</sup>, those of temperate landscapes are typically  $\sim 1$  km/km<sup>2</sup> [Kirkby, 1986].

[6] The main objective of this paper is to quantify how the ratio of sediment transport on hillslopes to sediment transport in channels influences the overall landscape morphology and dynamics. As indicated above, some aspects of this topic have already received investigation in the literature. This paper extends and unifies these studies within a consistent framework by clearly identifying any important controlling parameters and by systematically studying how the landscape morphology and dynamics vary as a function of these parameters. Our analysis includes the identification of a new nondimensional parameter  $D_e$  that is a function of rainfall, system size, rock type and hydraulic regime and that is a measure of the relative importance of fluvial and hillslope sediment transport. We show that  $D_e$  has an important influence on the surface morphology, channel network form, channel spacing (or drainage density) and the time scale of surface evolution. We quantify results by analyzing exposed surface area (reflecting surface roughness), channel sinuosity (reflecting how the channel network is organized on the surface), interface width or root-mean-square height fluctuation (reflecting roughness and relief), and crossover length scales (reflecting the average channel spacing). The scaling behavior of simulated topography with respect to both time and space is obtained. In addition, surface and channel network morphologies are shown to be strongly influenced by the overall surface slope relative to the magnitude of initial topographic roughness.

[7] The approach taken in this study is to numerically solve and investigate solutions of equations that are based on the conservation of surface water and sediment combined with a simple transport law connecting the sediment flux to the local slope and runoff discharge. This formulation is due largely to Smith and Bretherton [1972] and is similar to the equations studied by Córdova *et al.* [1982], Loewenherz-Lawrence [1994], and Smith *et al.* [1997a, 1997b]. The governing equations are solved here by the finite element method.

## 2. Governing Equations

[8] The formulation considered consists of two equations for the two unknown functions  $h(x, y, t)$  and  $q(x, y, t)$ , the surface elevation and the magnitude of the surface fluid discharge per unit width, respectively [see Smith and Bretherton, 1972]. These equations are derived by assuming that the masses of moving sediment and surface water are conserved:

$$\frac{\partial h}{\partial t} = -\nabla \cdot (\mathbf{n} q_s) \quad (1)$$

$$\nabla \cdot (\mathbf{n} q) = \alpha, \quad (2)$$

where  $\mathbf{n}$  ( $= -\nabla h/S$ ) is a unit vector directed down the surface gradient,  $S$  is the local slope of the surface ( $= |\nabla h|$ ),  $\alpha$  ( $>0$  and assumed to be spatially constant) is the effective rainfall (the average rainfall in excess of infiltration) and  $q_s$  is the sediment discharge per unit width (see Table 1 for notation). Note that  $\mathbf{q}_s$  and  $\mathbf{q}$  are the vector fields  $\mathbf{n}q_s$  and  $\mathbf{n}q$ , respectively. The symbols  $\nabla \cdot$  and  $\nabla$  represent the divergence and the gradient operators, respectively. Equation (1) indicates that the time rate of change in surface elevation is balanced by the divergence of the sediment discharge, while equation (2) indicates that fluid from steady rainfall flows off the surface as a gravity-driven flow directed down the local gradient. Neglect of the time derivative in equation (2) is made on the basis of the observation that the timescale of overland flow of runoff is generally far faster than the timescale associated with transport of topography (sediment) [see also *Smith et al.*, 1997b]. Relative base level changes (not included here) can be incorporated in the formulation either by including a source term in equation (1) or by directly constraining  $h$  on the desired boundary.

[9] The constitutive law for the sediment discharge can have a variety of forms depending on the geomorphologic/hydrologic setting and numerous different variations have been proposed [e.g., *Culling*, 1960; *Andrews and Bucknam*, 1987; *Graf*, 1971; *Smith and Bretherton*, 1972; *Kirkby*, 1986]. The approach taken here is to use one of the simplest physically reasonable laws that enable simultaneous development of both diffusive hillslopes and an incisive drainage network and to apply this law to the entire surface without distinction or prespecification of channel and hillslope regions. This law can be written as

$$q_s = \kappa S + c q^n S \quad (3)$$

where  $\kappa$  is the hillslope diffusivity,  $c$  is the fluvial transport coefficient, and  $n$  is a power law exponent quantifying the dependency of sediment transport on fluid discharge. The first term represents the widely accepted dependency of sediment flux on local slope [*Culling*, 1960] whereas the second term is included to account for fluvial transport [*Graf*, 1971]. Note that by proposing this transport law, it is assumed that the system is transport-limited, meaning that there is no limit imposed by the supply of sediment (see discussions by *Culling* [1965], *Carson and Kirkby* [1972], and *Howard* [1994]). Note also that no distinction is made here between suspended and bed load transport. In this sense, the fluvial term in equation (3) is intended to approximate the total fluvial load [see also *Smith and Bretherton*, 1972]. Many total transport laws assume a nonlinear dependency of sediment flux on slope. Inclusion of such a dependency in equation (3) is likely to modify surface and channel properties (e.g., channel concavity) but will lead to the same type of general behavior (i.e., nonlinear diffusion). An obvious and easily justifiable addition to equation (3) would be to include a threshold below which discharge-assisted sediment transport is negligible, for which considerable experimental and theoretical support exists [*Graf*, 1971]. A second possible addition would be to include a term whereby the hillslope sediment flux increases rapidly as a critical slope is approached, which has been suggested to capture some basic aspects of landsliding [see *Andrews and Bucknam*, 1987; *Roering et al.*, 2001].

**Table 1.** Notation

Symbol	Unit	Definition
$h$	m	surface elevation
$q$	$\text{m}^2 \text{s}^{-1}$	surface fluid discharge
$q_s$	$\text{m}^2 \text{s}^{-1}$	sediment discharge
$x, y$	m	horizontal coordinates
$t$	s	time
$S$	—	slope of local topography ( $=  \nabla h $ $= \sqrt{(\partial h/\partial x)^2 + (\partial h/\partial y)^2}$ )
$\alpha$	$\text{m s}^{-1}$	effective rainfall
$\kappa$	$\text{m}^2 \text{s}^{-1}$	substrate diffusion coefficient
$c$	$(\text{m}^2 \text{s}^{-1})/(\text{m}^2 \text{s}^{-1})^n$	coefficient for discharge-dependent sediment transport
$n$	—	exponent for dependency of fluid discharge on sediment transport
$L$	m	characteristic horizontal dimension (slope width perpendicular to ridge)
$\tilde{t}$	—	dimensionless time ( $= t \kappa/L^2$ )
$\tilde{x}, \tilde{y}$	—	dimensionless distances ( $= x/L, y/L$ )
$\tilde{h}$	—	dimensionless elevation ( $= h/L$ )
$\tilde{q}$	—	dimensionless fluid discharge ( $= q/(\alpha L)$ )
$D_e$	—	dimensionless diffusion parameter ( $= c \alpha^n L^n/\kappa$ )
$h_r$	—	maximum initial value of random noise
$H$	—	initial topographic height at ridge axis
$\lambda$	—	dimensionless roughness ( $= h_r/H$ )

[10] It is noteworthy that the adopted transport law is written in terms of sediment discharge per unit width  $q_s$  ( $\text{m}^2 \text{s}^{-1}$ ) rather than the total sediment discharge  $Q_s$  ( $\text{m}^3 \text{s}^{-1}$ ), the two being related by  $Q_s = \int_0^W q_s dW$  (where  $W$  is the channel width). This formulation is useful because it avoids the explicit introduction of a channel width and is natural given the form of the continuity equation for fluid (also written in terms of discharge per unit width). The reader is referred to *Tucker and Slingerland* [1997] for an example of a more typical formulation involving explicit relationships between water flux, channel width and water depth.

[11] Substituting equation (3) into equation (1), the system of governing equations can be rewritten as

$$\frac{\partial h}{\partial t} = \nabla \cdot ((\kappa + c q^n) \nabla h) \quad (4)$$

$$\nabla \cdot \left( \frac{\nabla h}{|\nabla h|} q \right) = -\alpha. \quad (5)$$

Equation (4) is recognized as a transient nonlinear diffusion equation while equation (5) is a steady nonlinear advection equation. Note that the grouping  $\kappa + c q^n$  in equation (4) has the role and dimensions of a diffusion coefficient (that can vary in time and space). The entirely diffusive nature of (4) is reflected by the terminology adopted within this study whereby transport processes have been separated for discussion purposes into “dispersive” and “concentrative” components [see also *Howard*, 1994], as opposed to the terms “diffusive” and “advective” more commonly used in the literature. The dispersive and concentrative processes are sometimes also simply referred to as “hillslope” and “fluvial”, respectively, due to their respective dominance in these landscape settings.

[12] This study treats the governing equations in their nondimensional form. This has the advantage that the



number of independent parameters appearing in the governing equations can be reduced from four (i.e.,  $\kappa$ ,  $c$ ,  $\alpha$ , and  $n$ ) to two, which greatly facilitates sensitivity analysis. Natural scales for nondimensionalization of equations (4) and (5) are the linear diffusion timescale  $t^*$ , the characteristic length scale  $L$  (e.g., horizontal slope length), and the fluid discharge at the characteristic length scale  $Q^*$ . One may introduce

$$t = \tilde{t} t^* = \tilde{t} L^2 / \kappa,$$

$$h = \tilde{h} L, \quad x = \tilde{x} L, \quad y = \tilde{y} L,$$

$$q = \tilde{q} Q^* = \tilde{q} \alpha L,$$

where dimensionless quantities are indicated by tilde symbols. Substituting these expressions into equations (4) and (5) yields the dimensionless equations

$$\frac{\partial \tilde{h}}{\partial \tilde{t}} = \tilde{\nabla} \cdot ((1 + D_e \tilde{q}^n) \tilde{\nabla} \tilde{h}) \quad (6)$$

$$\tilde{\nabla} \cdot \left( \frac{\tilde{\nabla} \tilde{h}}{|\tilde{\nabla} \tilde{h}|} \tilde{q} \right) = -1, \quad (7)$$

and the dimensionless parameter

$$D_e = \frac{c \alpha^n L^n}{\kappa}. \quad (8)$$

The parameter  $D_e$  is a measure of the relative importance of dispersive processes related to hillslope creep versus concentrative processes related to water-assisted transport acting on the landscape. If  $D_e \ll 1$ , nonlinear diffusion due to the dependency of the diffusion coefficient on runoff dominates over linear diffusion associated with hillslope creep. If  $D_e \gg 1$  the dependency of the diffusion coefficient on runoff is negligible and topographic evolution reduces to a linear equation controlled by hillslope creep. An alternative interpretation of  $D_e$  can be made by defining the characteristic timescales of hillslope and fluvial processes as  $\tau_h = L^2 / \kappa$  and  $\tau_f = L^2 / (c \alpha^n L^n)$ , respectively, where  $D_e$  can be written as the ratio of the two timescales  $\tau_h / \tau_f$ . Note that  $D_e$  is not an erosion Péclet number since there is strictly no advective sediment transport. Similar nondimensional formulations for erosion have been presented by *Smith and Bretherton* [1972], *Willgoose et al.* [1991b], and *Smith et al.* [1997a]. A parameter very similar (though not exactly equivalent) to  $D_e$  was derived by *Willgoose et al.* [1991b, equation 27]. Differences between the two nondimensional parameters are due to differences in the governing equations and in the characteristic scales adopted.

### 3. Numerical Method and Approach

[13] Equations (6) and (7) form a closed system of coupled nonlinear equations that are solved in a classical manner by the finite element method on an irregular triangular mesh [*Zienkiewicz and Taylor*, 2000a]. Equation (6) is discretized using the Galerkin method with cubic

shape and weighting functions using 7-node triangles. Equation (7) is discretized on 3-node triangles using linear shape functions and streamline (upwind) Petrov-Galerkin weighting [*Zienkiewicz and Taylor*, 2000b] in order to suppress numerical oscillations associated with strong advection. This procedure involves the addition of anisotropic diffusion to regions where the Péclet number locally exceeds unity, which has the effect of preventing infinite concentration of flow in channels, a problem known to exist with equation (7) [see *Izumi and Parker*, 1995]. The added artificial diffusion mimics real physical processes (e.g., eddy viscosity) that have similar stabilizing effects in the Navier-Stokes equations but which have been eliminated in the simplified formulation adopted. Locations with zero local slopes are singular (see equation (7)) and are treated by setting the fluid flux to zero. Discretization in time was performed using linear explicit finite differences while nonlinearities in both equations are treated by lagging solution-dependent coefficients by one time step.

[14] All results presented were performed on a two-dimensional spatial domain discretized by  $\sim 20,000$  elements. This number proved to be sufficient in order to resolve the major channel structures but is unlikely to capture structure beyond channel orders of 4–5. Higher-resolution simulations capable in future studies are anticipated to reveal more fine-scale channel structure and sharper channel-hillslope boundaries but are not anticipated to influence landscape dynamics. Dynamic behavior (such as anastomosing channel networks and stream capture events) observed in simulations (see section 4.1) persist as the time step increment is decreased, indicating that these features are unlikely to be numerical artifacts.

[15] Note that a far more commonly applied approach to solving the general coupled erosion problem is to use a discrete routing algorithm [e.g., *Chase*, 1992]. While many variants of this method have been developed and applied the general strategy involves progressively routing material (both sediment and fluid) down the computed drainage network between nearest discrete neighbors from the highest to the lowest elevation. This strategy differs from the continuum approach adopted here [see also *Smith et al.*, 1997b] in which sediment and fluid implicitly move down the local surface gradient. The discrete routing approach has an advantage over the continuum approach in that it is computationally efficient but it suffers from a grid dependency introduced by routing between a single nearest neighbor. In principal, this numerical artifact could be eliminated by redistributing fluid among neighboring cells according to the local gradient. An alternative approach is to mask the artifact using high resolution and/or an irregular spatial grid [*Braun and Sambridge*, 1997]. The continuum approach has the advantage that grid dependency is reduced and that the routing of sediment and fluid is achieved automatically as a result of the discretization and solution process rather than manually on the basis of some user-defined redistribution algorithm. The disadvantage of the adopted approach is greater computational expense.

### 4. Results

[16] Numerical solutions of equations (6) and (7) were computed to investigate erosion of, and runoff over a

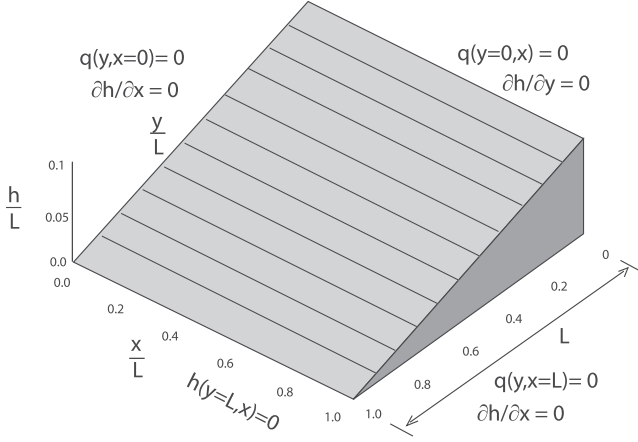


**Figure 1.** Initial topographic surface and boundary conditions used in computations. The surface has an initial slope of 1/10 unless stated otherwise. A random perturbation (i.e., roughness) is added to this surface to localize runoff. The influence of the magnitude of initial roughness on subsequent landscape evolution is investigated in section 4.4 and Figure 7.

simple, initially unchannelled, tilted, planar topographic surface perturbed by gaussian random noise (Figure 1). Boundary conditions consist of (1) a symmetrical ridge crest with zero water and sediment flux, (2) zero sediment and water flux normal to lateral boundaries, and (3) fixed topographic elevation at the slope base. Note that these boundary conditions imply that the system is open with respect to transport of sediment and fluid.

[17] Attention is focused on landscape development and morphology as a function of both time and  $D_e$  with constant values for the power exponent  $n$  ( $= 2$ ). This value, which is consistent with experimental data [see *Graf, 1971*], implies that sediment discharge is strongly dependent on the runoff discharge. Note that when  $n \leq 1$ , channelization does not occur in the continuum formulation because the relative sediment carrying capacity does not increase when initial perturbations induce flow convergence [see *Smith and Bretherton, 1972*]. A number of studies have shown that varying  $n$  (or similarly the area-slope exponent) has a large influence on valley profile concavity and on the general landscape form [e.g., see *Tucker and Whipple, 2002*].

[18] The morphology of simulated surfaces is quantified by determining the root-mean-square height fluctuation or interface width  $\tilde{w}$  (reflecting the surface roughness, relief and interface scaling properties), the exposed surface area  $\tilde{A}$  (reflecting the surface roughness) and the channel sinuosity (reflecting how the channel network is organized on the topography). One-dimensional profiles are determined by interpolating from the irregular triangular mesh to a regular cellular mesh with an approximately equivalent resolution (i.e.,  $\sim 150 \times 150$ ). The nondimensional interface width is defined as [e.g., *Barabási and Stanley, 1995*]

$$\tilde{w}(\tilde{l}, \tilde{t}) = w/L = \frac{1}{L} \sqrt{\langle [h(\tilde{x}, \tilde{t}) - h_l(\tilde{x}, \tilde{t})]^2 \rangle_x}. \quad (9)$$

The subscript  $l$  means that a single window of data with length  $l$  is selected in the direction parallel to the ridge axis

and used to measure the interface width and mean height  $h_l(\tilde{x}, \tilde{t})$  in this window. The angle brackets  $\langle \rangle_x$  denote that averages are taken over  $x$ . Many different windows along the same ridge-parallel profile are taken and the result is averaged to obtain  $\tilde{w}(\tilde{l}, \tilde{t})$ . The mean interface width  $\hat{\tilde{w}}$  is obtained by taking the mean of  $\tilde{w}$  measured in many different ridge-parallel profiles. Note that although the interface width (as formulated here) is a 1-D measure, it contains information from the entire 2-D surface. The interface width, in addition to giving information concerning the surface roughness and relief, is also used to measure the roughness exponent (describing how the interface width scales with the window size), and to quantify the dominant channel spacing, since the interface width saturates (does not increase further) once the window size exceeds the channel spacing. The nondimensional exposed surface area is defined as

$$\tilde{A} = A/A_o = \sum_{j=1}^{N_j} \sqrt{1 + S_j^2}, \quad (10)$$

where  $S_j$  is the average slope of an element  $j$ ,  $N_j$  is the total number of elements,  $A$  is the total surface area and  $A_o$  is the initial total surface area. The average slope of an element is calculated as the average of slopes determined at nodes using the piecewise element shape function derivatives. The nondimensional channel sinuosity (or average channel length) is defined here as

$$S_e = \frac{1}{N_i} \sum_{i=1}^{N_i} \frac{l_{si}}{l_{oi}}, \quad (11)$$

where  $l_{si}$  is the length of stream  $i$ ,  $l_{oi}$  is the length of stream  $i$  from source to outlet in a straight line, and  $N_i$  is the total number of streams sampled. The channel sinuosity was calculated by specifying arbitrary channel sources in a reasonably regular fashion over the entire grid and by tracing each “stream” to its respective outlet. Note that this method does not require actual definition of channels (and their sources) and can easily be carried out automatically by stream tracing down local gradients. In this respect, the measure may be best thought of as a flow sinuosity rather than a channel sinuosity.

#### 4.1. General Surface Evolution

[19] The first results to be presented demonstrate general features of how topography and runoff evolve through time for relatively high  $D_e$  in response to constant climatic forcing in the form of uniform steady rainfall (Figure 2). Note that because base level is maintained at a constant level throughout all simulations (i.e., the surface is not undergoing uplift) the steady state solution is a flat surface that has been completely eroded.

[20] The initial stage of topographic development is governed by the presence and magnitude of initial topographic perturbations (roughness) that have the ability to inhibit accumulation of runoff. Thus, even though  $D_e$  has a large value indicating an overall dominance of runoff-assisted sediment transport (at the slope length scale  $L$ ), the pinning of runoff at a scale much shorter than the slope length scale effectively means that initial topographic evo-

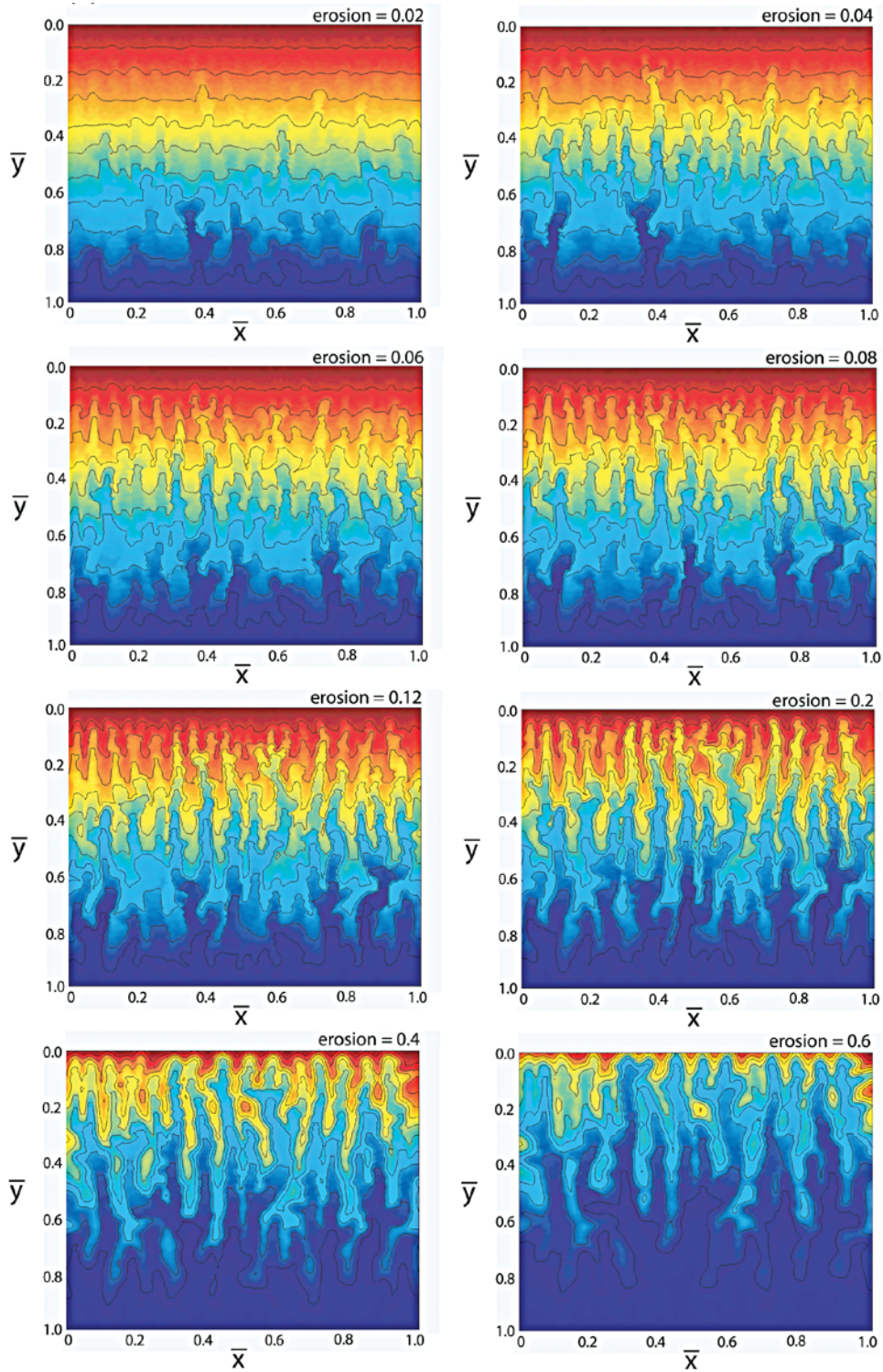


**Figure 2a.** Contour plots showing how topography evolves through time in response to constant base level (calculated for  $D_e = 10^3$ ,  $n = 2$  and  $\lambda = 1$ ; see equation (12)). The values of erosion shown above each box represent the total erosion which has taken place since the experiment was initiated. Thus an erosion of 0.0 represents the initial conditions whereas a value of 1.0 indicates the time when all of the initial topography has been removed. An erosion of 1.0 also coincides with the steady state solution.



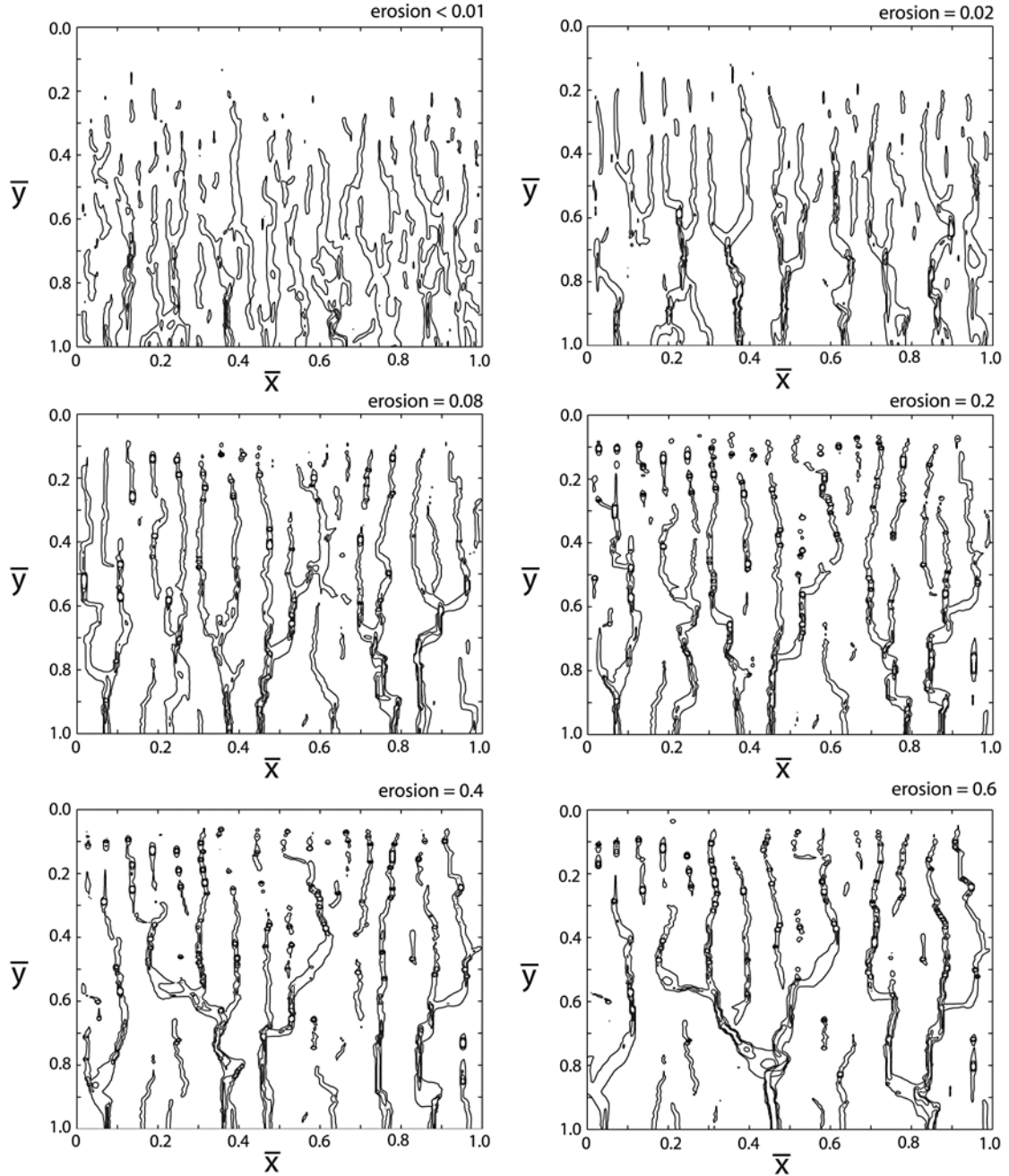


**Figure 2b.** Same as Figure 2a except runoff discharge.

lution is governed by linear diffusion (since  $\tilde{q}$  is small). This is particularly true when the initial surface is relatively flat and/or the magnitude of initial roughness is large. The initially formed channel network has an anastomosing form (e.g., before 0.02 erosion in Figure 2b) that migrates laterally in an unstable fashion. However, with increasing time, diffusion (both dispersive and concentrative) efficiently decays initial roughness due to its short-wavelength nature allowing runoff to coalesce into larger streams and for concentrative sediment transport to increase in importance relative to dispersive transport. This leads to the formation of more stable channels (e.g., after 0.2 erosion in Figure 2b) which further concentrate runoff giving rise to positive feedback and enhanced channel incision.

[21] Several major changes in surface morphology take place in response to erosion and the development of a fully developed channel network in the simulations investigated. First, the average channel spacing (quantified as the cross-over length scale in Figure 3a) first decreases and then slowly increases in a quasi-linear fashion. Second, incision causes the overall surface roughness (or total exposed surface area) to increase sharply before attaining a maximum and decreasing in an exponential fashion (Figure 3b). Together, these observations imply a two-phase stage of topographic evolution. Surface morphology during the initial (growth) phase reflects the fact that new channels are rapidly formed and propagate headward toward the upper boundary. In the later (decay) phase, topographic

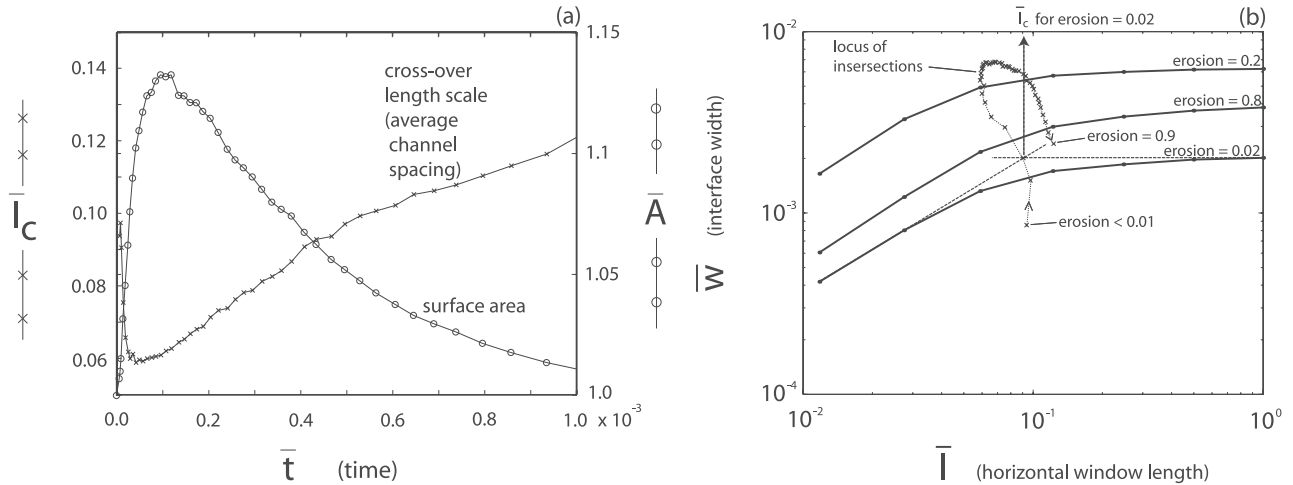


**Figure 3.** (a) Evolution of the exposed surface area  $\tilde{A}$  (surface roughness) and the crossover length scale  $\tilde{l}_c$  (average channel spacing) for the simulation shown in Figure 2 ( $D_e = 10^3$ ,  $n = 2$  and  $\lambda = 1$ ). The exposed surface area is determined from equation (10). (b) Calculation of the crossover length scale. For every time of interest, corresponding to a fixed proportion of erosion, the scaling between the interface width  $\tilde{w}$  and the spatial window size  $\tilde{l}$  is determined via equation (9) (three examples of such scaling relations are shown in Figure 3b). The crossover length scale  $\tilde{l}_c$  corresponds to the length scale at which the interface width saturates (or ceases to further increase). This value is obtained as the intersection between two straight lines (shown in Figure 3b for erosion of 0.02). Also shown in Figure 3b is the locus of how the intersections (i.e., the value  $\tilde{l}_c$ ) vary through time. This locus of intersections is plotted in Figure 3a as the crossover length scale versus time. Note that the crossover length scale shown in Figure 3b also corresponds to the average channel spacing, since the interface width determined in the direction parallel to the ridge axis saturates once the window size reaches the channel spacing.

evolution is dominated by lateral and vertical incision within the already existing channel network. Interestingly, deposition does not play a major role in the topographic evolution. This is due largely to imposition of a fixed lower topographic boundary condition.

[22] The transition from a growth to a decay phase of landscape evolution can be interpreted as a saturation phenomenon related to the progressive development of spatial correlations. During the initial stage of erosion, different parts of the topographic surface act largely independently of one another and depend mainly on local properties (local slope and hillslope diffusivity). This stage, which is dominated by linear diffusion, is characterized by a short correlation length, the magnitude of which is controlled mainly by initial topographic perturbations. As erosion proceeds, runoff of fluid over the surface and associated fluvial sediment transport transmits information about the surface properties over a progressively larger area. Thus, even though erosion occurs locally, the increase in correlation length enables lateral spread of information that is manifest in the surface as headward incision. When the correlation length reaches the size of the system, corresponding to the arrival of headward incision at the upper boundary, the surface properties (e.g., the surface area) saturates. Subsequent evolution evolves by the progressive decay of topography developed prior to saturation rather than by the formation of new features. Note that although the initial stage of topographic development, as represented by the depinning of runoff trapped on the surface by topographic perturbations and the transition through anastomosing to a fully developed channel net-

work, is short-lived and involves a small amount of total erosion, it represents an important period in the overall landscape development because it involves the formation of channels, the location of which tend to remain relatively stable throughout subsequent evolution.

#### 4.2. Influence of $D_e$ on Landscape Morphology

[23] Simulations indicate that  $D_e$ , a measure of the relative importance of dispersive hillslope and concentrative fluvial transport processes, exerts an important influence on landscape morphology. Large values of  $D_e$  (i.e., sediment transport is dominated by concentrative fluvial processes) favor development of rough, highly incised topography and a dense, branched channel network, whereas lowering the value of  $D_e$ , corresponding to increasing the contribution to sediment transport from dispersive hillslope processes, results in smoother topography and straighter, less branched channels that have a greater average spacing (Figure 4). For the maximum value of  $D_e$  investigated (i.e., 10,000), the maximum exposed surface area  $\tilde{A}_{\max}$  (i.e., the surface area at saturation) and the channel sinuosity (or equivalently the average channel length) are both enhanced by  $\sim 30\%$  relative to low values of  $D_e$  (Figures 5a and 5b). The average channel spacing (as reflected by the crossover length scale  $\tilde{l}_c$ ) varies from a minimum value of  $\sim \tilde{l}_c = 0.05$  corresponding to  $\sim 20$  channels per unit length at  $D_e = 10,000$  to infinity at  $D_e \leq 1$  (i.e., no channelization observed). Together, these results are consistent with the widely accepted notion that increasing the importance of dispersive sediment transport tends to suppress channel incision [e.g., Dunne and Aubry, 1986; Loewenherz-Law-



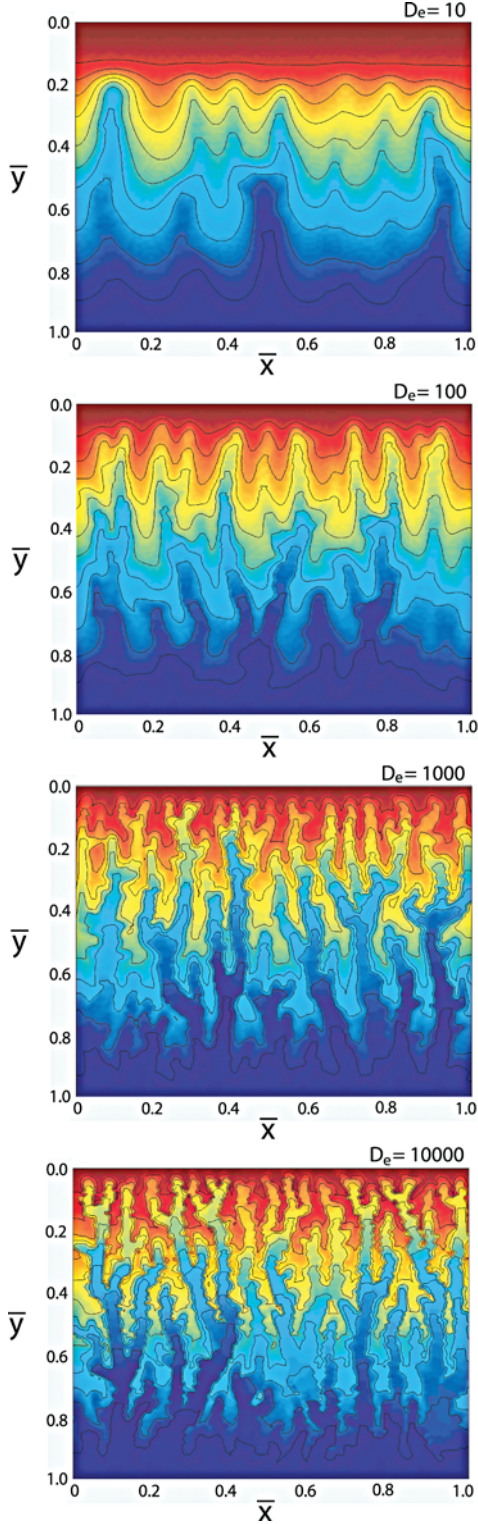


**Figure 4.** Influence of  $D_e$  on surface morphology (erosion of 0.2,  $n = 2$ ,  $\lambda = 1$ ). Large values of  $D_e$  indicate sediment transport is dominated by fluvial processes, whereas for small  $D_e$ , hillslope sediment transport becomes more important.

rence, 1994] and to decrease the channel density [e.g., Kirkby, 1986; Tarboton et al., 1992; Willgoose et al., 1992].

[24] The relationship between the interface width  $\tilde{w}$  and the window length  $\tilde{l}$  in the region below crossover is of the

approximate form  $w \propto l^\gamma$  where the roughness exponent  $\gamma$  is  $\sim 0.8$  (Figure 5d). This roughness exponent is within the range of values measured for natural topography [see Dodds and Rothman, 2000]. Note that the magnitude of  $D_e$  exerts no influence on the spatial scaling of the interface width (i.e., on  $\gamma$ ) while it has an important control on the ultimate magnitude of the width.

### 4.3. Influence of $D_e$ on Landscape Dynamics

[25] The magnitude of  $D_e$  exerts an important influence on landscape dynamics. For example, increasing  $D_e$  results in a decrease in the timescale within which a landscape responds to erosion, due to an increase in the bulk diffusivity of the system. The response to increasing  $D_e$  is recognized in landscapes by an increase in the rate of surface roughening during the growth phase of topographic evolution associated with more rapid vertical and headward incision and an increase in the rate of surface smoothing during the decay phase (Figure 6a). The relationship between the timescale required for saturation  $\tilde{t}_s$  and  $D_e$  is observed to have the approximate form  $\tilde{t}_s \propto D_e^{-0.78}$  (Figure 6b). Thus increasing  $D_e$  by a factor of 10 decreases the response time of the system by a factor of  $\sim 6$ . This result demonstrates the ability of fluvial processes to greatly increase rates of topographic evolution.

[26] It is interesting to note that roughening of the surface does not lead to power law scaling with time, as is observed for most surface evolution processes [e.g., see Barabási and Stanley, 1995]. The time evolution of the surface morphology properties such as interface width  $\tilde{w}$  follows a logarithmic-type law during the growth phase (i.e., the positive part of the curve in Figure 6c) of the approximate form  $\tilde{w} \propto m \log \tilde{t}$  (where  $m$  is the slope on a linear log plot). The reason for this difference may lie in the unstable nature of initial channel incision that generates an exponential increase in roughness at small times. This result implies that the classic growth exponent is not well defined.

### 4.4. Effects Due to Variations in Initial Surface Conditions

[27] Given that initial stages of surface evolution are strongly influenced by the presence and magnitude of initial roughness (see section 4.1), it is anticipated that the initial surface geometry may have an important influence on finite landscape morphologies. Indeed, a considerable amount of work has already demonstrated that variability in the randomness applied as initial conditions can result in significant variations in the form and statistics of channel networks [e.g., Willgoose et al., 1991b; Howard, 1994]. Attention here is focused on a different effect, namely that due to variations in the relative magnitude of initial noise. This effect has been tested in simulations carried out with different values of the dimensionless parameter

$$\lambda = h_r/H, \quad (12)$$

where  $h_r$  is the maximum value of initial random noise and  $H$  is the surface height at the ridge axis. Note that  $\lambda \rightarrow \infty$  as the regional slope approaches zero. Results show that  $\lambda$  has a strong influence on the form of the channel network, with small values of  $\lambda$  (corresponding to a steep overall slope and/or a small magnitude of initial roughness) favoring

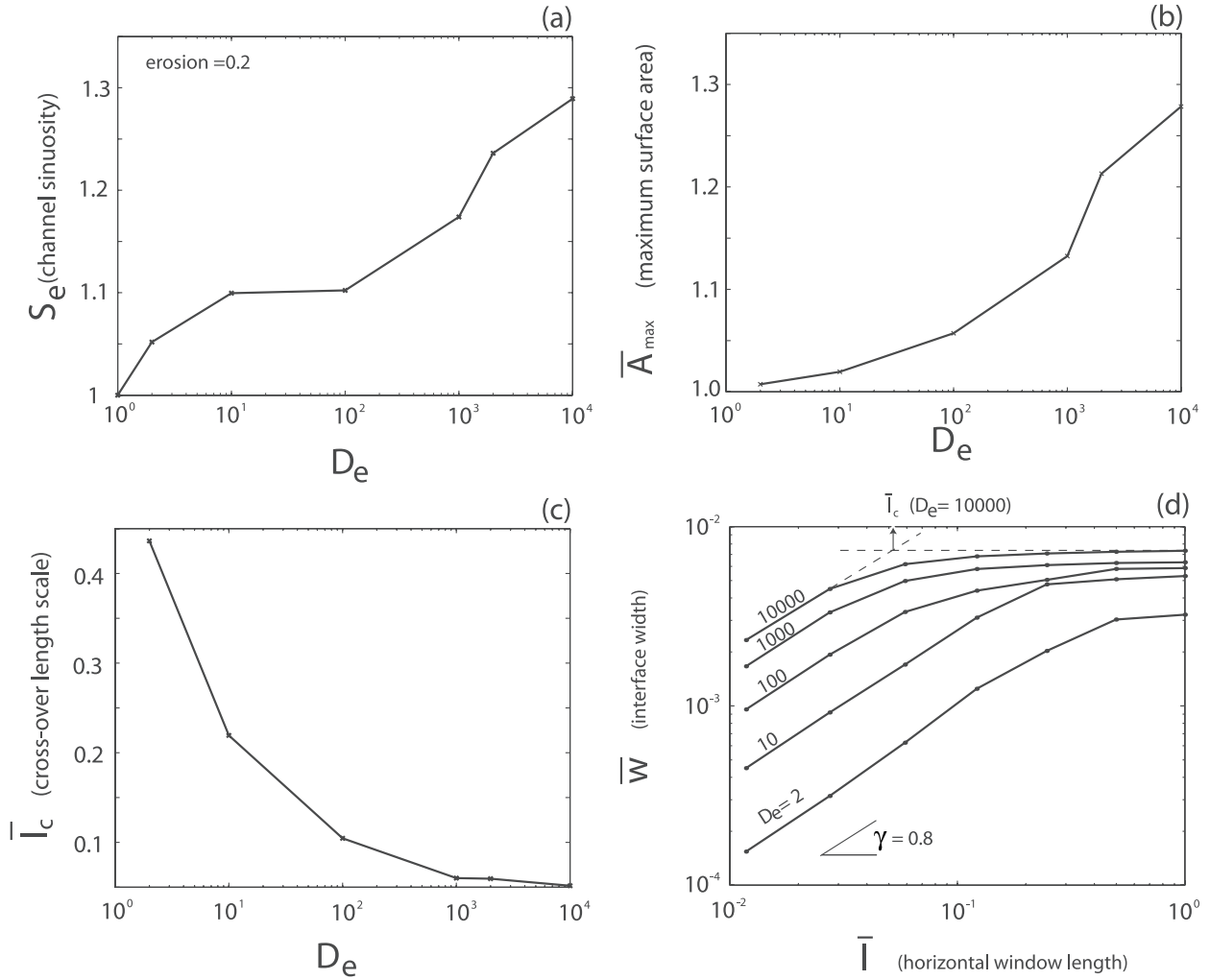


**Figure 5.** Influence of  $D_e$  on (a) channel sinuosity, (b) maximum exposed surface area, (c) crossover length scale (average channel spacing, and (d) interface width scaling. Channel sinuosity, as defined here, is determined from equation (11). This figure indicates that the ratio of fluvial to hillslope sediment transport (i.e.,  $D_e$ ) has an important influence on surface and channel network properties.

parallel drainage networks and an almost periodic channel spacing (e.g., Figure 7a), whereas large values of  $\lambda$  favor development of highly branched channel networks (e.g., Figure 7d). These results are consistent with field observations showing that dendritic drainage networks tend to develop in regions with gentle slopes whereas parallel drainage networks are characteristic of moderate or steep regional slopes [e.g., Howard, 1967]. The influence of  $\lambda$  increases sharply for values greater than  $\sim 10$ , as indicated by a dramatic ( $\sim 50\%$ ) increase in channel sinuosity or average channel length as the relative magnitude of roughness is increased further (Figure 8a).

[28] It is interesting to note the apparent increase in the scale of observation as  $\lambda$  is increased (i.e., Figure 7a resembles small-scale rill structures on a hillslope, whereas Figure 7d resembles a large-scale drainage pattern). This effect, although not due to a change in scale, may actually reflect one, since at the scale of a single hillslope (in natural systems) the ridge height tends to be large relative to the magnitude of roughness whereas at larger scales the regional slope becomes progressively smaller relative to rough-

ness. As discussed more in section 5, this interpretation has interesting implications concerning the dependency of channel morphology on scale.

[29] Varying the relative magnitude of initial noise also influences the interface width, with large magnitudes of  $\lambda$  causing large interface widths or relatively rough surfaces (Figure 8b). A more surprising result is that  $\lambda$  significantly influences the interface scaling. The roughness exponents increase from  $\sim 0.7$  to  $\sim 0.8$  as  $\lambda$  is increased from 0.1 to 100 (Figure 8b). Note that  $\lambda$  does not influence the crossover length scale (Figure 8b) or equivalently the characteristic drainage spacing (Figure 7).

[30] The reason for the observed dependency of the channel network form on  $\lambda$  is likely to be due to the influence of surface roughness on local flow directions. When a surface is relatively rough with stochastic noise (as is a surface which is flat on average), runoff flowing down the surface is strongly perturbed resulting in a highly branching channel network, whereas when the magnitude of roughness is relatively small (as is a steeply tilted surface), flow of runoff is relatively unhindered and the resulting

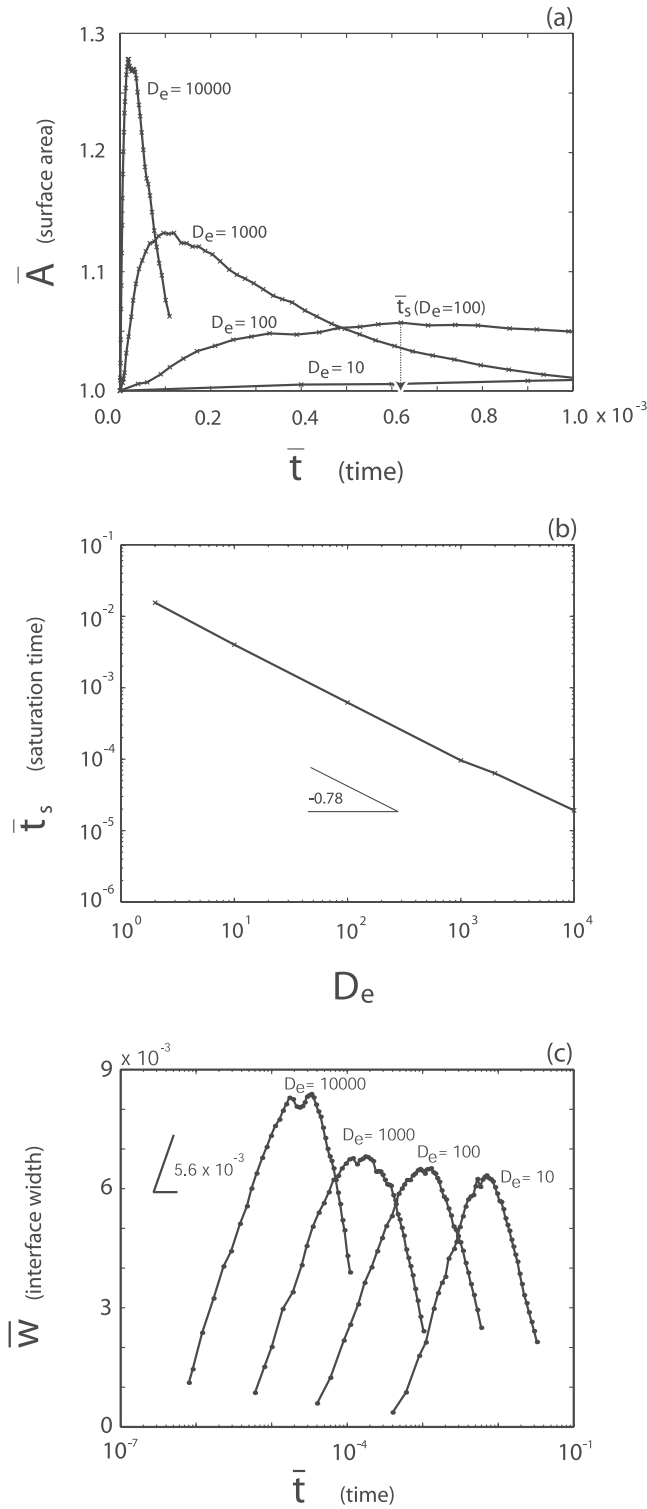


**Figure 6.** Influence of  $D_e$  on (a) the time evolution of surface area, (b) saturation time  $\bar{t}_s$ , and (c) interface width. The saturation time is defined as the time when the surface area saturates (as shown in Figure 6a for  $D_e = 100$ ). Note the linear relations between interface width and the logarithm of time during growth and decay phases (Figure 6c).

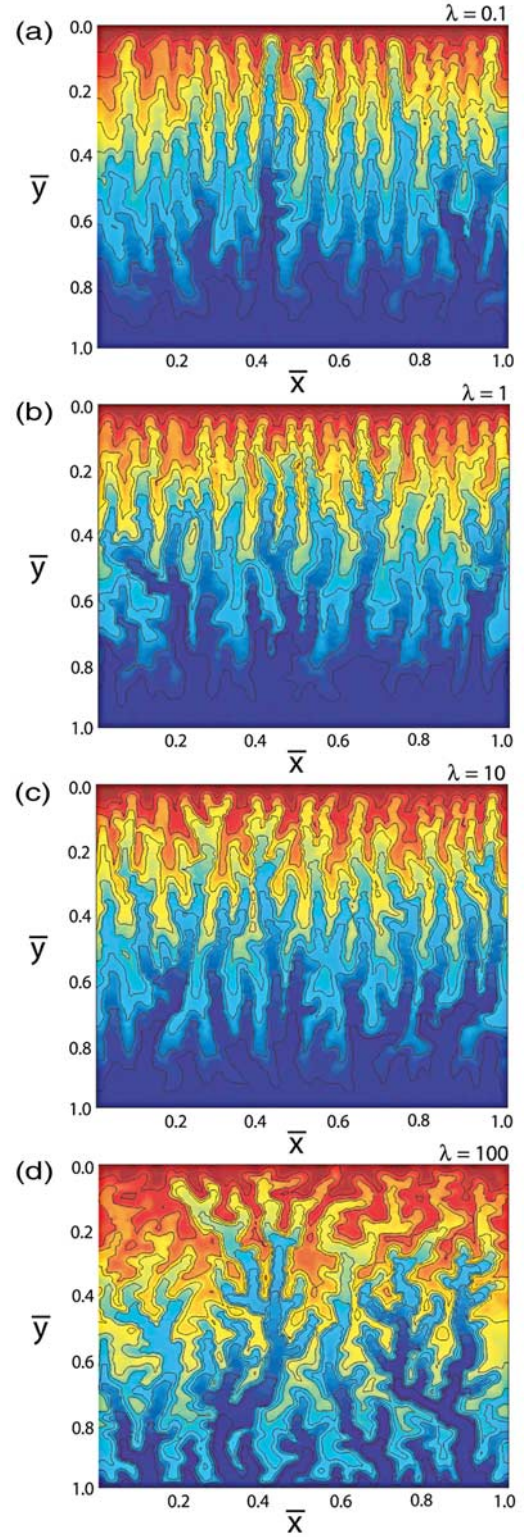


**Figure 7.** Influence of the relative magnitude of initial roughness ( $\lambda$ , see equation (12)) on surface morphologies ( $D_e = 1000$ ,  $n = 2$ , initial surface slope of  $1/100$ , erosion of  $0.2$ ). Small values of  $\lambda$  correspond to steep initial surfaces and/or small magnitude of initial roughness, whereas large values of  $\lambda$  correspond to flat initial surfaces and/or large magnitudes of initial roughness.



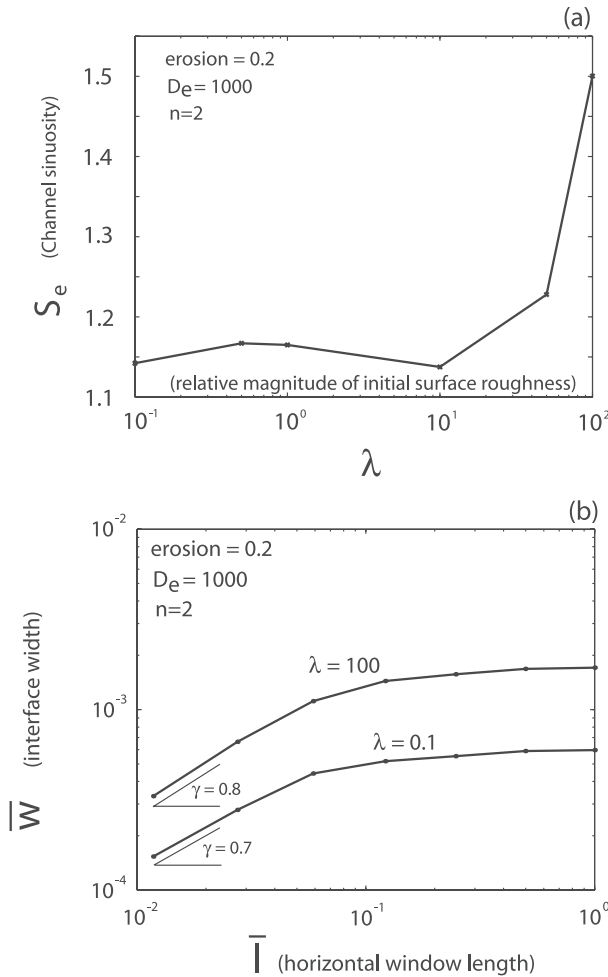


**Figure 8.** Influence of  $\lambda$  (the relative magnitude of initial roughness) on (a) channel sinuosity  $S_e$  (see equation (11)) and (b) interface width scaling for two of the simulations shown in Figure 7.

channel network tends to be more regular and parallel in nature. Note that in the extreme case where the magnitude of initial roughness is zero (and the initial surface is exactly planar), no channelization occurs and the solutions become truly one-dimensional (i.e., neither the discharge or topography exhibit variation parallel to the ridge axis).

## 5. Discussion

[31] One of the major objectives of this study has been to systematically investigate how the ratio of sediment transport on hillslopes to sediment transport in channels influences the overall landscape morphology and dynamics. To this end, we have derived a critical nondimensional number  $D_e$  which can be interpreted as the ratio of characteristic timescales associated with dispersive and concentrative sediment transport processes, respectively. This number is a function of other parameters such as the characteristic system size (or slope length), hillslope diffusivity, fluvial detachment coefficient, steady state rainfall and hydraulic regime.  $D_e$  is the only independent parameter (apart from those related to initial conditions) which can influence

landscape evolution for the set of equations investigated. Simulations demonstrate that  $D_e$  has an important influence on both surface and channel network morphology and the response time of landscapes, with large values of  $D_e$  (i.e., fluvial-dominated sediment transport) favoring rough highly incised surfaces containing a dense (closely spaced) channel network that evolves rapidly in time. For lower values of  $D_e$ , time evolution is slower, the resulting landscapes are smoother and the channel network is less branching and less dense. Note that high steady state rainfall (large  $D_e$ ) corresponds to fluvial-dominated model landscapes (Figure 4), whereas in nature it is typical that relatively dry climates with highly sporadic rainfall are fluvial-dominated. Thus equating “strongly fluvial” and “wet” is not possible. This point emphasizes the importance of considering transient effects of climate when estimating values of  $D_e$  from natural landscapes. The importance of a transient climate in influencing erosion rates has been argued by *Molnar* [2001] on the basis of general transport laws and the frequency-magnitude distribution of floods and has been investigated numerically by *Tucker and Bras* [2000].

[32] Our results imply that some important properties of landscapes such as local relief, drainage density and exposed surface area are strongly influenced by the dominant process of sediment transport. In particular, fluvial-dominated systems favor generation of large relief (i.e., large interface widths) and large total exposed surface area. We emphasize that even though it is river channels which are capable of creating large relief, hillslope sediment transport imposes an important limit to the total relief through modifying the hillslope length and channel density [see also *Montgomery and Dietrich*, 1992]. Thus the finite landscape morphology reflects the relative importance of sediment transport processes: competition between the roughening influence of concentrative fluvial transport and the smoothing influence of hillslope transport. Interestingly, the increase in surface area due to fluvial incision may have a self-regulating influence on landscape morphology by increasing the proportion of substrate available for (weathering and) hillslope transport. Thus the effective magnitude of  $D_e$  may be buffered by the landscape. This effect may explain why the channel spacing (and to a lesser extent the exposed surface area) saturates with increasing  $D_e$  beyond  $\sim 10^3$  (see Figures 5b and 5c).

[33] The predictable way in which landscape morphology responds to  $D_e$  is broadly consistent with other studies. For example, field-based studies indicate that hillslopes tend to dominate landscapes at small spatial scales (small  $D_e$ ), whereas fluvial features tend to dominate at large scales (large  $D_e$ ) (e.g., *Montgomery and Dietrich*, 1992). Furthermore, whereas high drainage densities (and small channel spacings) are often found in association with semiarid badland-type (fluvial dominated) landscapes, low drainage densities (large channel spacings) are typical of more humid (hillslope dominated) landscapes [e.g., *Kirkby*, 1992]. Similarly, many studies have shown that catchment properties such as the areas-slope relationship are strongly influenced by the ratio between the importance of hillslope and channel processes, the transition (in process dominance) being controlled by change of scale [e.g., *Willgoose*, 1994], rock type [e.g., *Howard*, 1994], climate [e.g., *Tucker and Sling-*

erland, 1997], or the presence of different dominant hillslope processes [e.g., Tucker and Bras, 1998]. A major contribution of this study has been to put results such as these into a consistent framework by identifying a single independent controlling parameter (i.e.,  $D_e$ , which depends on all other model parameters) and by quantifying its influence.

[34] The strong dependency of average channel spacing on  $D_e$  demonstrated here is inconsistent with field data presented by Hovius [1996], at least at first glance. Hovius [1996] showed that major rivers draining relatively linear mountain belts from around the world display a remarkably regular spacing in a wide range of climatic settings and substrate lithologies. The same data also show a consistent linear relationship between drainage spacing and the half width of the mountain belt, implying a strong kinematic or geometrical control on the spacing of major rivers (in well-developed drainage systems). In contrast, simulations indicate that the average channel spacing tends to decrease with increasing  $D_e$ , and therefore with increasing system size. However, the connection between this study and that of Hovius [1996] is not straightforward since attention here is focused on the average channel spacing, not the spacing of major drainage outlets as investigated by Hovius [1996]. The two measures yield significantly different results as illustrated in Figure 2b (erosion is 0.6), where it can be seen that there are 2–3 major drainage outlets (with a spacing of  $\sim 0.5$ ), but where the calculated average channel spacing is 0.084 (implying  $1/0.084 \approx 12$  channels). In this case, the empirical relation of Hovius [1996] predicts a spacing of 0.5, as observed for major channel outlets (given that the width of the slope is 1). An additional complication is implied by the observation that the channel structure and spacing changes in time (e.g., in Figure 2b compare erosion is 0.02 where there is a single channel spacing frequency with erosion of 0.6 which shows an additional channel frequency at larger scale comprising the “major” drainage outlets). Together these observations highlight the difficulty of resolving the channel spacing problem as currently posed and the importance of devising measures (e.g., analyzing spectra or interface width crossover distances) that can be applied to large data sets in an objective fashion.

[35] It is interesting to note that the characteristic timescale for linear hillslope processes based on the relation  $\tau_h = L^2/\kappa$  varies between  $\sim 1000$  and  $10,000$  Ma for a hillslope diffusivity  $10^3 \text{ m}^2 \text{ Ma}^{-1}$  [e.g., Hanks et al., 1984] and systems sizes varying between 1 and 10 km, respectively. The enormity of this timescale compared to the time within which landscapes are thought to respond may tempt one to argue that linear hillslope diffusion of regolith or other cohesionless material makes up a negligible contribution to natural landscapes and can, therefore, be ignored. However, as our simulations demonstrate, both the landscape morphology and dynamics are sensitive to variations in  $D_e$ , even for large values of  $D_e$  corresponding to small hillslope diffusivities. The inclusion of fluvial sediment transport drastically decreases the timescale of landscape evolution. For example, increasing  $D_e$  by a factor of 10 decreases the system response time by a factor of 6 assuming  $n = 2$  (see section 4.3). This result implies that in order for landscapes at spatial scales of 1 to 10 km to evolve on timescales of 1 Ma,  $D_e$  must be on the order of  $1000\text{--}10,000$  (based on

the hillslope timescale discussed above). A  $D_e$  of this magnitude appears at least plausible based on the visual appearance of model landscapes (see Figure 4). Note that the fluvial transport exponent  $n$  will strongly influence the rate of topographic evolution, with fast response times corresponding to large values of  $n$ . The surface morphology and channel spacing are less sensitive to varying  $n$ , as long as  $n > 1$ .

[36] Treating landscapes as a transport-limited system involving coupling between hillslope and fluvial processes leads naturally to the clear identification of an effective (system) diffusivity  $\kappa_e = \kappa + c q^n$  (see equation (4)), or in non dimensional form  $\tilde{\kappa}_e = 1 + D_e \tilde{q}^n$  (see equation (6)). As noted above, because  $\kappa_e$  increases with system size (due to dependency of  $\kappa_e$  on  $q$ ), the time scale within which finite landscapes develop is considerably smaller than the case for systems evolving by pure linear diffusion. In reality,  $\kappa_e$  is a function of the frequency and magnitude of rainfall (only the latter of which has been treated here). Estimation of the effective diffusivity (and therefore of the system sediment transport function) in natural systems could potentially be obtained by measuring (at a variety of length scales) system response times related to either climatic or tectonic perturbations.

[37] Results of simulations demonstrate that landscapes undergo important changes in surface and channel network morphology as erosion proceeds with time. For example, it was shown that following the emergence of highly dynamic shallow incisions on an initially unchannelled surface, the channel network stabilizes and develops by a combination of headward incision and lateral channel widening. These features appear to be reasonably well understood and have been observed in many numerical studies [e.g., see Willgoose et al., 1991c; Rigon et al., 1994; Tucker and Slingerland, 1997]. The general coarsening of natural drainage networks with time does not appear to have been widely discussed in the literature, although it has been observed [e.g., Collins et al., 1983; Smith et al., 1997b]. This behavior is interpreted to indicate a transition between an early (linear) development stage where incisive instabilities are fast growing and of very short wavelength and later development (nonlinear) stages where slower growing, longer wavelength instabilities begin to dominate due to saturation of earlier instabilities, as theoretical results suggest [e.g., Loewenherz-Lawrence, 1994]. If this interpretation is correct, one may expect in nature that short-wavelength channel features to have small amplitudes (because they saturate early) and long-wavelength features to have relatively large amplitudes. This inference is consistent with studies showing that natural landscapes tend to be self-similar [e.g., Huang and Turcotte, 1989] and with the observed power law scaling between  $\tilde{w}$  and  $\tilde{l}$  (e.g., Figure 5d). Note, however, that short-wavelength channels are anticipated to be difficult to observe in humid climates with abundant soil cover because response times are so rapid at small scales that channels formed in early development stages are likely to be rapidly obliterated during periods of prolonged precipitation. The exception to this may occur in relatively arid climates during erosion in response to short and intense rain bursts. Early stages of topographic development bearing very short wavelength incisions have more chance of being preserved due to the

sporadic nature of precipitation events that are separated by long periods within which very little erosion occurs because of an almost complete lack of hillslope diffusion.

[38] A characteristic feature demonstrated by the simulations presented is the presence of a two-stage history for landscape evolution (e.g., see Figure 3). Surface morphology during the initial (growth) phase reflects the fact that new channels are rapidly formed and propagate headward toward the upper boundary resulting in growth of relief and surface roughening. In the later (decay) phase, topographic evolution is dominated by lateral and vertical incision within the already existing channel network that leads to exponential decay of topographic relief and smoothing of topography toward a flat (steady state) surface. Similar phases of topographic evolution were envisaged by Davis [1954] and have commonly been observed in numerical models studying the response to impulse-like tectonic forcing [e.g., Willgoose, 1994; Kooi and Beaumont, 1996; Smith *et al.*, 1997b], although these studies distinguished three rather than two main phases. We suggest that the transition from growth to decay phases of topographic evolution is explained by the growth of spatial correlations on the surface, which eventually reach the system size at which time the entire surface becomes correlated and the surface properties (such as interface width) saturate (see section 4.1 for more detail). This interpretation is consistent with the observed dependency of the time required for saturation (i.e.,  $\tilde{t}_s$ ) on  $D_e$  and with the general observation that saturation coincides with the arrival of backward incision at the upper boundary (e.g., erosion of 0.2 in Figure 2). Kooi and Beaumont [1996] suggest that the transition from growing to declining sediment yield indicates the time when rivers achieve grade at the base level for the first time, at which time a local dynamic equilibrium is achieved. However, these authors also point out that this dynamic equilibrium cannot correspond to overall macroscopic equilibrium since the latter coincides with steady state when all topography is eroded to base level (i.e., assuming zero base level change following initial block uplift). An interesting question that needs to be addressed in future work is: Does the saturation time related to channels connecting with the entire surface correspond with the time at which steady state is achieved in situations experiencing constant base level fall?

[39] Simulations demonstrate that some important features of landscapes form very early in the erosional history, reflecting an important dependence on initial conditions. This result is illustrated by the formation of channels during the initial growth phase of topographic evolution, the location of which remain relatively constant throughout subsequent evolution (Figure 2b) and by the strong influence that the magnitude of initial roughness (relative to the overall surface slope) has on finite surface and channel network morphologies (Figure 7). Similar interpretations have been made on the basis of field data. For example, it is well known that dendritic drainage networks tend to develop in regions with gentle initial slopes whereas parallel drainage networks are characteristic of moderate or steep regional slopes [e.g., Howard, 1967]. Furthermore, Talling *et al.* [1997] argue that the drainage spacing may be determined primarily during the early stages of channel network growth. We suggest that the dependency of surface

and channel network morphologies on initial noise is related to competition between the local roughening effect of noise and global smoothing effect of diffusive sediment transport. In this sense, the initial topographic noise acts as a form of quenched noise except that it is progressively decayed in time by diffusion. If the noise is initially large, then it can significantly influence the flow directions and the channel network before time has had a chance to eliminate its influence. If, on the other hand, the initial noise is relatively small, the surface and channel network morphology is determined largely by competition between dispersive and concentrative sediment transport. Simulations indicate that the effect of increasing the magnitude of initial roughness appears similar to the effect that could be anticipated by increasing the scale of observation (see section 4.4). We suggest that this effect, although not due to a change in scale, may actually reflect one, since casual observation of natural examples indicates that, at the scale of a single hillslope, the ridge height tends to be large relative to the magnitude of roughness (a condition tending to favor the formation of rill-like channels) whereas at larger scales, regionally averaged slopes become progressively smaller relative to roughness (a condition leading to the formation of more complex dendritic drainage networks). It is suggested that structures such as rills are not necessarily restricted to small scale (i.e., because of some specific process dominance at this scale) but that the initial surface conditions favorable for their formation tend to be typical at small scale. Similar arguments apply to the formation of large-scale dendritic drainage basins. Thus we argue for a continuous transition between, and a single formation mode for small-scale structures such as rills and large-scale drainage basins.

[40] This paper has also quantified how interface width scales as a function of space and time. Roughness exponents derived from simulations, which describe how the interface width changes with changing spatial scale, vary between 0.7 and 0.8 at small scales. These exponents progressively decrease as scale increases, before eventually dropping close to zero at the scale defined by the main channel spacing (termed here the crossover length scale). Similar exponents and crossover behavior are reported for natural data [e.g., Dodds and Rothman, 2000]. Model roughness exponents at the smallest scale are shown to be independent of  $D_e$ , which is a surprising result given the strong influence  $D_e$  imposes on the overall surface properties. Nevertheless, this result is consistent with the work of Rigon *et al.* [1994], who showed the scaling of planar properties (such as interface width) does not appear to be significantly influenced by hillslope diffusion, whereas the scaling of surface properties is modified. The roughness exponents are, however, dependent on the relative magnitude of initial noise. A similar dependency of roughness exponents on noise has been observed for many other physical systems [Barabási and Stanley, 1995]. Willgoose *et al.* [1991b] also showed that network statistics (such as the length and bifurcation ratios) are sensitive to small variations of initial randomness (while holding the magnitude of noise constant). Note however, that such variations lead to networks that are “physically similar” [see also Howard, 1994], which is not the case when varying the magnitude of initial noise (see Figure 7). A surprising result found here is the logarithmic



scaling observed between interface width and time. Physically this law implies that the interface width initially grows very rapidly while later it grows very slowly. As suggested in section 4.3, the reason for this behavior may lie in the initially unstable nature of channel incision [see *Smith and Bretherton*, 1972; *Loewenherz-Lawrence*, 1994] that generates a rapid increase in roughness at small times. It is much more normal that surface growth in other physical systems is controlled by power laws [*Barabási and Stanley*, 1995]. That fact that growth of surfaces by erosion is not controlled by a power law indicates that the growth exponent is not defined.

## 6. Conclusions

[41] This paper presented a detailed investigation of how the ratio of sediment transport on hillslopes to sediment transport in channels influences landscape and channel network morphology and dynamics. This problem has been investigated by numerically solving and investigating solutions of equations that are based on the conservation of surface water and sediment combined with a simple transport law connecting the sediment flux to the local slope and runoff discharge. The most important points of this study are summarized as follows:

[42] 1. We have identified a critical nondimensional parameter  $D_e$  that is a function of rainfall, system size, rock type and hydraulic regime and that is a measure of the relative importance of fluvial and hillslope sediment transport. Large values of  $D_e$  imply that sediment transport is dominantly fluvial.  $D_e$  is the only independent parameter (apart from those related to initial conditions) which can influence landscape evolution for the set of equations investigated.

[43] 2.  $D_e$  has an important and predictable influence on the surface morphology (e.g., total exposed surface area, surface roughness, local relief), channel network form (e.g., channel sinuosity), and channel spacing. Fluvial dominated systems (i.e., large  $D_e$ ) are characterized by rough, high-relief, highly incised surfaces which contain a dense (closely spaced) channel network. Lowering  $D_e$  leads to smoother topography, lower-relief, greater channel spacing and less sinuous channels.

[44] 3.  $D_e$  has an important influence on the dynamics of erosion, with large values of  $D_e$  greatly increasing the rate at which landscapes evolve.

[45] 4. Topographic evolution in the absence of base level change tends to occur in two major phases, an initial growth phase reflecting formation of new channel and creation of relief and a later decay phase related to destruction of preexisting channels. The transition between growth and decay phases is suggested to be related to a saturation phenomenon.

[46] 5. The scaling behavior of simulated topography with respect to both time and space is obtained and is shown to be independent of  $D_e$ . Roughness exponents are found to be in the range 0.7–0.8. The magnitude of initial roughness influences the roughness exponents. The interface width is shown to grow and decay as the logarithm of time. Thus the classical growth exponent is undefined.

[47] 6. Surface and channel network morphologies are shown to be strongly influenced by the overall surface slope

relative to the magnitude of initial topographic roughness (with relatively flat and/or rough initial surfaces favoring development of highly branching channel networks, whereas relatively steep initial surfaces favor parallel drainage patterns with regular drainage spacings).

[48] Finally, this study indirectly shows that classical well-established numerical techniques such as the finite element method can be used with success to investigate the coupled runoff-erosion problem.

[49] **Acknowledgments.** Yuri Podladchikov, Alex Densmore, and Mike Ellis are thanked for providing encouragement and for many stimulating discussions. Reviews and comments by Clem Chase, Kelin Whipple, and two anonymous reviewers are greatly appreciated. This work was supported by the Swiss National Science Foundation (grant 620-57863).

## References

- Ahnert, F., Process-response models of denudation at different spatial scales, *Catena Suppl.*, 10, 31–50, 1987.
- Andrews, D. J., and R. C. Bucknam, Fitting degradation of shoreline scarps by a nonlinear diffusion model, *J. Geophys. Res.*, 92, 12,857–12,867, 1987.
- Barabási, A.-L., and H. E. Stanley, *Fractal Concepts in Surface Growth*, 366 pp., Cambridge Univ. Press, New York, 1995.
- Beaumont, C., P. Fullsack, and J. Hamilton, Erosional control of active compressional orogens, in *Thrust Tectonics*, edited by K. R. McClay, pp. 1–18, Chapman and Hall, New York, 1992.
- Braun, J., and M. Sambridge, Modeling landscape evolution on geological time scales: A new method based on irregular spatial discretisation, *Basin Res.*, 9, 27–52, 1997.
- Carson, M. A., and M. J. Kirkby, *Hillslope Form and Process*, 475 pp., Cambridge Univ. Press, New York, 1972.
- Chase, C. G., Fluvial landsculpting and the fractal dimension of topography, *Geomorphology*, 5, 39–57, 1992.
- Collins, B. D., T. Dunne, and A. K. Lehre, Erosion of tephra-covered hillslopes north of Mt St. Helens, Washington: May 1980–May 1981, *Z. Geomorphol., Suppl.*, 46, 103–121, 1983.
- Córdova, J. R., I. Rodríguez-Iturbe, and P. Vaca, On the development of drainage networks, in *Recent Developments in the Explanation and Prediction of Erosion and Sediment Yield*, edited by D. E. Walling, IAHS Publ., 137, 239–249, 1982.
- Culling, W. E. H., Analytical theory of erosion, *J. Geol.*, 68, 336–344, 1960.
- Culling, W. E. H., Theory of erosion on soil-covered slopes, *J. Geol.*, 73, 230–254, 1965.
- Davis, W. M., *Geographical Essays*, 777 pp., Dover, Mineola, N.Y., 1954.
- Dodds, P. S., and D. H. Rothman, Scaling, universality and geomorphology, *Annu. Rev. Earth Planet. Sci.*, 28, 571–610, 2000.
- Dunne, T., and B. A. Aubry, Evaluation of Horton's theory of sheetwash and rill erosion on the basis of field experiments, in *Hillslope Processes, Binghamton Symp. Geomorphol. Int. Ser.*, vol. 16, edited by A. D. Abrahams, pp. 31–53, Allen and Unwin, Concord, Mass., 1986.
- Graf, W. H., *Hydraulics of Sediment Transport*, 513 pp., McGraw-Hill, New York, 1971.
- Hanks, T. C., R. C. Bucknam, K. R. Lajoie, and R. F. Wallace, Modification of wave-cut and faulting-controlled landforms, *J. Geophys. Res.*, 89, 5771–5790, 1984.
- Hasbargen, L. E., and C. Paola, Landscape instability in an experimental drainage basin, *Geology*, 28, 1067–1070, 2000.
- Horton, R. E., Erosional development of streams and their drainage basins: Hydrophysical approach to quantitative morphology, *Geol. Soc. Am. Bull.*, 56, 275–370, 1945.
- Hovius, N., Regular spacing of drainage outlets from linear mountain belts, *Basin Res.*, 8, 29–44, 1996.
- Howard, A. D., Drainage analysis in geologic interpretation: A summary, *Am. Assoc. Pet. Geol. Bull.*, 51, 2246–2259, 1967.
- Howard, A. D., A detachment-limited model of drainage basin evolution, *Water Resour. Res.*, 30, 2261–2285, 1994.
- Huang, J., and D. L. Turcotte, Fractal mapping of digitized images: Applications to the topography of Arizona and comparison with synthetic images, *J. Geophys. Res.*, 94, 7491–7495, 1989.
- Izumi, N., and G. Parker, Inception of channelization and drainage basin formation: Upstream-driven theory, *J. Fluid Mech.*, 283, 341–363, 1995.
- Izumi, N., and G. Parker, Linear stability analysis of channel inception: Downstream-driven theory, *J. Fluid Mech.*, 419, 239–262, 2000.

- Kirkby, M. J., A two-dimensional simulation model for slope and stream evolution, in *Hillslope Processes, Binghamton Symp. Geomorphol. Int. Ser.*, vol. 16, edited by A. D. Abrahams, pp. 203–222, Allen and Unwin, Concord, Mass., 1986.
- Kirkby, M. J., Thresholds and instability in stream head hollows: A model of magnitude and frequency for wash processes, in *Process Models and Theoretical Geomorphology*, edited by M. J. Kirkby, pp. 295–314, John Wiley, New York, 1994.
- Kooi, H., and C. Beaumont, Escarpment evolution on high-elevation rifted margins: Insights derived from a surface evolution model that combines diffusion, advection and reaction, *J. Geophys. Res.*, 99, 12,191–12,209, 1994.
- Kooi, H., and C. Beaumont, Large-scale geomorphology: classical concepts reconciled and integrated with contemporary ideas via a surface processes model, *J. Geophys. Res.*, 101, 3361–3386, 1996.
- Loewenherz-Lawrence, D. S., Hydrodynamic description for advective sediment transport processes and rill initiation, *Water Resour. Res.*, 30, 3203–3212, 1994.
- Molnar, P., Climate change, flooding in arid environments, and erosion rates, *Geology*, 29, 1071–1074, 2001.
- Montgomery, D. R., and W. E. Dietrich, Channel initiation and the problem of landscape scale, *Science*, 255, 826–830, 1992.
- Rigon, R., A. Rinaldo, and I. Rodriguez-Iturbe, On landscape evolution, *J. Geophys. Res.*, 99, 11,971–11,993, 1994.
- Rinaldo, A., W. E. Dietrich, R. Rigon, G. Vogel, and I. Rodriguez-Iturbe, Geomorphological signatures of varying climate, *Nature*, 374, 632–634, 1995.
- Roering, J. J., J. W. Kirchner, and W. E. Dietrich, Hillslope evolution by nonlinear, slope-dependent transport: Steady state morphology and equilibrium adjustment timescales, *J. Geophys. Res.*, 106, 16,499–16,513, 2001.
- Schumm, S. A., Evolution of drainage systems and slopes in badlands at Perth Amboy, New Jersey, *Geol. Soc. Am. Bull.*, 67, 597–646, 1956.
- Smith, T. R., and F. P. Bretherton, Stability and the conservation of mass in drainage basin evolution, *Water Resour. Res.*, 8, 1506–1529, 1972.
- Smith, T. R., B. Birnir, and G. E. Merchant, Towards an elementary theory of drainage basin evolution: I, The theoretical basis, *Comput. Geosci.*, 23, 811–822, 1997a.
- Smith, T. R., G. E. Merchant, and B. Birnir, Towards an elementary theory of drainage basin evolution: I, Computational evaluation, *Comput. Geosci.*, 23, 823–849, 1997b.
- Talling, P. J., M. D. Stewart, C. P. Stark, S. Gupta, and S. J. Vincent, Regular spacing of drainage outlets from linear fault blocks, *Basin Res.*, 9, 275–302, 1997.
- Tarboton, D. G., R. L. Bras, and I. Rodriguez-Iturbe, A physical basis for drainage density, *Geomorphology*, 5, 59–76, 1992.
- Tucker, G. E., and R. L. Bras, Hillslope processes, drainage density, and landscape morphology, *Water Resour. Res.*, 34, 2751–2764, 1998.
- Tucker, G. E., and R. L. Bras, A stochastic approach to modeling the role of rainfall variability in drainage basin evolution, *Water Resour. Res.*, 36, 1953–1964, 2000.
- Tucker, G. E., and R. Slingerland, Erosional dynamics, flexural isostasy, and long-lived escarpments: A numerical modeling study, *J. Geophys. Res.*, 99, 12,229–12,243, 1994.
- Tucker, G. E., and R. Slingerland, Drainage basin response to climate change, *Water Resour. Res.*, 33, 2031–2047, 1997.
- Tucker, G. E., and K. X. Whipple, Topographic outcomes predicted by stream erosion models: Sensitivity analysis and intermodel comparison, *J. Geophys. Res.*, 107, 2179, doi:10.1029/2001JB000162, 2002.
- Willett, S. D., R. Slingerland, and N. Hovius, Uplift, Shortening and Steady State Topography in Active Mountain Belts, *Am. J. Sci.*, 301, 455–485, 2001.
- Willgoose, G., A physical explanation for an observed area-slope-elevation relationship for catchments with declining relief, *Water Resour. Res.*, 30, 151–159, 1994.
- Willgoose, G. R., R. L. Bras, and I. Rodriguez-Iturbe, A coupled channel network and hillslope evolution model: 1. Theory, *Water Resour. Res.*, 27, 1671–1684, 1991a.
- Willgoose, G. R., R. L. Bras, and I. Rodriguez-Iturbe, A coupled channel network and hillslope evolution model: 2. Nondimensionalization and applications, *Water Resour. Res.*, 27, 1685–1696, 1991b.
- Willgoose, G. R., R. L. Bras, and I. Rodriguez-Iturbe, Results from a new model of river basin evolution, *Earth Surf. Processes Landforms*, 16, 237–254, 1991c.
- Willgoose, G. R., R. L. Bras, and I. Rodriguez-Iturbe, A physical explanation of an observed link area-slope relationship, *Water Resour. Res.*, 27, 1697–1702, 1991d.
- Willgoose, G. R., R. L. Bras, and I. Rodriguez-Iturbe, The relationship between catchment and hillslope properties: Implications of a catchment evolution model, *Geomorphology*, 5, 21–37, 1992.
- Zienkiewicz, O. C., and R. L. Taylor, *The Finite Element Method*, vol. 1, *The Basis*, Butterworth-Heinemann, Woburn, Mass., 2000a.
- Zienkiewicz, O. C., and R. L. Taylor, *The Finite Element Method*, vol. 3, *Fluid dynamics*, Butterworth-Heinemann, Woburn, Mass., 2000b.

F. Schlunegger, Institute of Geological Sciences, University of Bern, Baltzerstr 1, Bern, CH-3012 Switzerland. (fritz.schlunegger@geo.unibe.ch)  
G. Simpson, Institut für Geologie, Sonneggstr. 5, ETH Zentrum, CH-8092 Zürich, Switzerland. (simpson@erdw.ethz.ch)